

A modified deep learning model in the classification of post-COVID-19 lung disease and a comparative study on Iranian and international databases

**S. Cheraghi^{1,2}, S. Amiri³, F. Abdolali⁴, A. Janati Esfahani^{5,6*},
A. Amiri Tehrani Zade^{7,8}, R. Ahadi⁹, F. Ansari², E. Raiesi Nafchi²,
Z. Hormozi-Moghaddam^{1,2}**

¹*Radiation Biology Research Center, Iran University of Medical Sciences, Tehran, Iran*

²*Department of Radiation Sciences, Allied Medicine Faculty, Iran University of Medical Sciences, Tehran, Iran*

³*Department of Computer Sciences, University of Copenhagen, Copenhagen, Denmark*

⁴*Department of Radiology and Diagnostic Imaging, Faculty of Medicine and Dentistry, Alberta University, Edmonton, AB, Canada*

⁵*Cellular and Molecular Research Center, Research Institute for Prevention of Non-Communicable Diseases, Qazvin University of Medical Sciences, Qazvin, Iran*

⁶*Department of medical biotechnology, School of advanced technologies in medicine, Qazvin University of Medical Sciences, Qazvin, Iran*

⁷*Department of Medical Physics and Biomedical Engineering, Tehran University of Medical Sciences (TUMS), Tehran, Iran*

⁸*Image-Guided Surgery Group, Research Centre for Biomedical Technologies and Robotics (RCBTR), Tehran University of Medical Sciences, Tehran, Iran*

⁹*Department of Anatomical Science Iran University of Medical Science Tehran, Iran*

ABSTRACT

► Original article

***Corresponding author:**

Azam Janati Esfahani, Ph.D.,

E-mail:

janaty.azam@gmail.com

Received: January 2023

Final revised: June 2023

Accepted: July 2023

*Int. J. Radiat. Res., January 2024;
22(1): 55-64*

DOI: 10.52547/ijrr.21.1.9

Keywords: Machine learning, COVID-19, Computed tomography, Mask R-CNN+CNN, Deep learning.

Background: We introduced Mask R-CNN+CNN as a deep learning model to classify COVID-19 and non-COVID-19 cases. Radiomic features relevant to COVID-19 was presented for Iranian and other nationalities. **Materials and Methods:** Chest CT images from 800 COVID-19 positive and negative patients were studied. The automated volume of the lung and segmentation of COVID-19 lung lesions were implemented using 3D U-net, Capsule network, and Mask R-CNN on annotated CT images. Deep learning models designed were based on Mask R-CNN, CNN, and Mask R-CNN+CNN algorithms to classify COVID-19 cases. We also explored radiomic features relevant to the COVID-19 pandemic in the lungs for chest CT images and implemented random forest (RF), decision tree (DT), and gradient boosting decision tree (GBDT) algorithms on two datasets. **Results:** The Mask R-CNN+CNN model demonstrated a higher classification accuracy (96.39 ± 2.94) compared to the Mask R-CNN and CNN models. The RF algorithm had greater power in differentiating relevant COVID-19 radiomic features compared to DT and GBDT, with an accuracy of at least 91 and an AUC of at least 985 in both datasets. We identified six radiomic features that were relevant to the pathological characteristics of COVID-19 positive/negative patients and were common across all datasets. **Conclusion:** This study emphasizes the power of Mask R-CNN+CNN with a ResNet-101 backbone as a CNN algorithm that utilizes bounding box offsets output from Mask R-CNN as the input for classifying COVID-19 cases. Radiomic features extracted from lung CT images might aid the diagnosis of COVID-19 in patients at various stages of the disease.

INTRODUCTION

The first cases of coronavirus disease 2019 (COVID-19) were observed in China in December 2019. COVID-19 rapidly spread worldwide and affected the healthcare systems of international communities⁽¹⁾. The main manifestation of COVID-19 is a severe viral infection that affects the respiratory system⁽²⁾. The lungs are the main organ affected by this acute viral infection. Based on pulmonary

symptoms and the risk of severe complications, including death, patients often require admission to the intensive care unit (ICU). Prevention of infection and disease through vaccination and early diagnosis remains crucial⁽³⁾. Although reverse-transcription polymerase chain reaction (RT-PCR) is the preferred test for COVID-19⁽⁴⁾, several studies have shown that chest computed tomography (CT) has a higher sensitivity of approximately 97% for COVID-19 than RT-PCR⁽⁵⁾. The competitive advantage and superior

performance of CT lie in its potential as a more powerful tool for management and decision-making regarding ICU treatment, as well as follow-up care for cases with ambiguous findings on chest X-rays (CXR) or positive RT-PCR test results (6-9), (8-10). Chest CT commonly reveals ground glass opacities (GGO), mixed GGOs, lung consolidation, crazy-paving patterns, bronchial dilation, peripheral distribution, interlobular septal thickening, and bilateral involvement (11-13) (6, 14). However, as the use of CT scan imaging increases, limitations are being observed in diagnosing lung lesions and differentiating types of pneumonia, depending on the conditions of the imaging system (15, 16). Moreover, some radiologists may not be experts in detecting infected regions (17). Consequently, it can be time-saving to have an automated tool to distinguish suspected areas in CT images. Numerous studies have been conducted on the use of artificial intelligence (AI) in medical diagnosis, and significant advances have been made in classifying images by convolutional neural networks (CNNs) (18).

Machine learning (ML) is a branch of artificial intelligence and computer science aiming to model complex relationships or patterns based on empirical data (19). Machine learning algorithms (MLAs) have demonstrated their good performance in situations involving the prediction of categories from spatially dispersed training data. They are particularly advantageous when a high-dimensional input space represents a complex investigative process. Given that chest CT is the most widely used diagnostic imaging modality for COVID-19, this study believes that medical image analysis utilizing artificial neural networks and ML techniques could be utilized to aid the early detection or identification of high-risk individuals (20).

In the current body of research, deep learning and ML approaches are widely employed to detect and segment regions of infected pneumonia, to reduce misdiagnosis and predict coronavirus infections based on medical image modalities (7, 20-23). These approaches can assist radiologists in enhancing their performance and making better decisions in managing the disease. In this regard, the support vector machine (SVM), gradient boosting machine (GBM), and random forest (RF) are the most frequently utilized machine learning methods (24).

Extracting precise information from medical images is a fundamental principle of radiomics modeling that leads to an accurate decision-making process in the diagnosis and treatment of diseases (25-28).

Medical images contain a wealth of information, and identifying their commonalities and divergences can help reduce uncertainties. This could lead to more targeted studies on both ML and deep learning. To obtain more accurate results, data should be gathered from various studies in different

communities to develop a comprehensive understanding of the pathogenesis pathways and treatment approaches. The reproducibility and consistency of radiomic features across multinational conditions and different images could contribute to the optimal use of medical imaging features in the diagnosis, prediction, and validation of modeling in all fields of research (30).

This study utilized international and Iranian datasets for COVID-19 classification to determine the most common radiomic features associated with the disease. A key objective was to propose a network that could be applied to different nationalities and CT scanners with varying protocols. Additionally, this study aimed to develop an intelligent model based on deep learning by collecting an extensive database of lung CT scan images and to examine its generalizability in classifying COVID-19 patients. We also assessed and compared the lung CT radiomic features associated with COVID-19 classification in both international and Iranian databases using ML algorithms. We hope to create an intelligent model based on the deep learning approach by compiling a large database of lung CT scan images and verifying its applicability for the classification of COVID-19 patients.

MATERIALS AND METHODS

This research was conducted in two steps. In the first step, two experienced and expert radiologists manually labeled each chest CT scan image as normal or abnormal for COVID-19 in International and Iranian datasets. The two radiologists were blinded to the patients' CT results. Additionally, they manually segmented the lung area and pulmonary lesions following COVID-19 from CT scans in the datasets. We used these segmentations to train the networks (as shown in figure 1). Three deep learning networks, namely Mask R-CNN (region-based convolution neural network), 3D U-Net, and Capsule network (Caps Net) were utilized to automatically segment lungs from CT scan images.

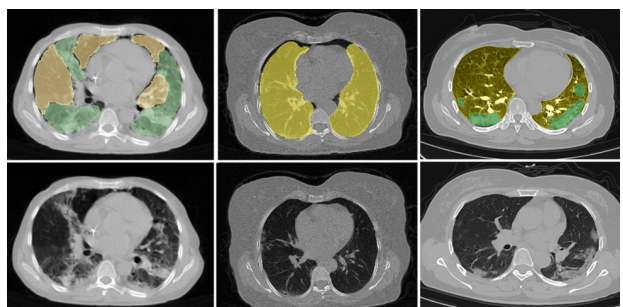


Figure 1. Normal and abnormal lung samples from 3 patients, the middle images show the normal lung and the left and right images show the involved lung. The yellow color in this figure shows the healthy areas, and the green color shows the affected areas.

After segmenting the lung area in all the samples, we classified them into normal or abnormal cases using three scenarios of Mask R-CNN, CNN, and Mask R-CNN+CNN algorithms. Mask R-CNN+CNN is a CNN algorithm that uses bonding box offsets output from Mask R-CNN as the input for class labeling. The automated bounding box generated by Mask R-CNN is based on what the radiologists annotated around the lung area in normal and abnormal samples. All three scenarios were implemented on three well-known architectures: dense convolutional networks (DenseNet-116), residual neural network (ResNet-50), and ResNet-101. Finally, we compared these three scenarios and presented the best model based on the evaluation results. The overall framework of our proposed technique is shown in figure 2.

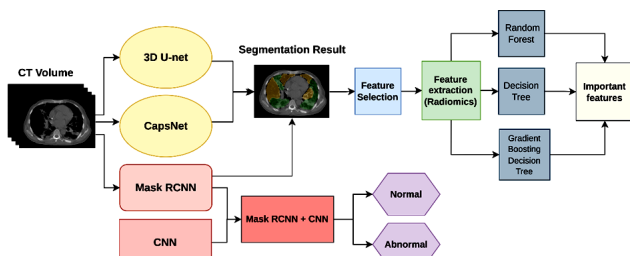


Figure 2. A detailed block diagram of the study in classification of COVID-19 lung disease and effective features extraction. Abbreviations: 3D U-net: three-dimensional U-shaped network architecture. CapsNet: Capsule network. Mask R-CNN: Mask region-based convolution neural network. CNN: Convolutional neural network. Mask RCNN+CNN is a CNN algorithm that uses bonding box offsets output from Mask-R CNN as input for class labeling.

Mask R-CNN is a deep neural network designed to address sample segmentation problems in machine learning, enabling the separation of different objects in an image. It provides object bounding boxes, classes, and masks when given an image. Mask R-CNN can be used in both training and testing phases. During the test phase, predicted boxes, masks, and class assurances are generated using the ground truth data (class labels, box coordinates, and masks) from the training phase. In this study, we used Mask R-CNN to determine the bounding box of standard and abnormal sample lungs as input for the Mask R-CNN+CNN algorithm for class labeling (figure 3).

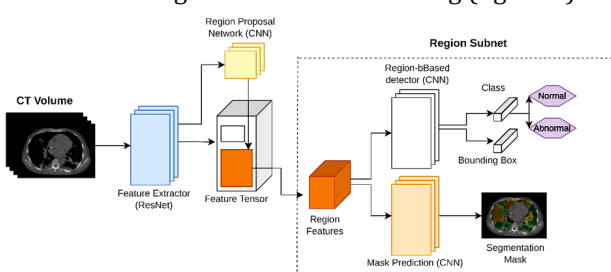


Figure 3. A detailed block diagram of the Mask R-CNN for COVID-19 image segmentation. Abbreviations: Mask R-CNN: Mask region-based convolution neural network. Resnet: Residual neural network. CNN: Convolutional neural network.

ResNet is the most widely used backbone for object detection and segmentation tasks (29). ResNet-101 is a convolutional neural network consisting of 101 deep layers, designed to aid in data classification. ResNet-50, which is a variant of the ResNet model trained on the ImageNet dataset, includes 48 convolution layers, one max pool layer, and one average pool layer. It has a total of 3.8×10^9 floating point operations.

DenseNet, which uses dense connections between layers, is similar to ResNet but with some significant differences. In DenseNet, the output of each layer is combined with the outputs of all preceding layers, whereas in ResNet, the output of each layer is added to the outputs of subsequent layers. This means that DenseNet creates a more direct path for gradient flow during training, which can help mitigate the vanishing gradient problem that can occur in very deep neural networks.

Radiomic features were extracted from the entire segmented lung volume in both COVID and non-COVID subjects. The extracted features were tagged as normal (non-COVID) or abnormal (COVID) in two separate groups, one international and one Iranian. Feature selection was performed using three techniques: select percentile, K-Best, and general univariate. Then, three classifiers, namely decision tree (DT), gradient boosting decision trees (GBDT), and random forest (RF), were used to determine feature importance. Finally, we compared the essential features of COVID-19 in both international and Iranian groups, and identified relevant common elements in the two datasets.

To the best of our knowledge, this is the first study to utilize machine learning models to compare the importance of COVID-19 features in both international and Iranian datasets, setting a precedent for future research in this domain.

Datasets

Our study analyzed 800 chest CT images, consisting of 200 scans from Iranian adult COVID-19 patients aged 18-80 years (113 females and 87 males), 200 scans from international (Italian, Chinese, Korean, and American) adult COVID-19 patients, and 400 healthy chest CT scans from both Iranian and non-Iranian individuals who were not infected with COVID-19.

The demographic information of Iranian patients is presented in Table 1. Prior to chest CT imaging, all COVID-19 positive patients had laboratory confirmation of their infection. This study focused on patients who experienced pulmonary complications following COVID-19, such as pneumonia, pleural effusion, bronchiectasis, dyspnea, chronic cough, and pulmonary fibrosis. The patients were examined approximately 2-3 weeks after PCR confirmation of their COVID-19 positivity. International data were collected from January 2020 to 2021 in many

datasets such as:

<http://medicalsegmentation.com/COVID19/>
<https://github.com/ThisIsIsaac/Data-Science-for-COVID-19>
<https://github.com/CSSEGISandData/COVID-19>
<https://dataVERSE.harvard.edu/dataset.xhtml?persistentId=doi:10.7910/DVN/6ACUZJ>
<https://www.kaggle.com/paultimothymooney/chest-xray>
<https://github.com/UCSD-AI4H/COVID-CT>
<https://github.com/CSSEGISandData/COVID-19>

Table 1. Iranian demographic data of all different age groups.

Patients Age	Number	Positive	Negative	Female	Male
18_19	18	11	7	7	11
20-30	52	25	27	30	22
31-40	47	28	19	21	26
41-50	62	27	35	29	33
51-60	67	29	38	39	28
61-70	77	36	41	39	38
71-80	77	44	33	46	31
Total	400	200	200	211	189

Iranian chest CT images were obtained using either a conventional spiral CT scanner (Neusoft CT-C3000, Neusoft Medical Systems, China) or a Siemens 16-slice CT scanner (SOMATOM Sensation 16, Siemens Healthcare, Germany).

High-resolution CT imaging was performed on Iranian patients using the following parameters: 120 kV; 80-100 mA; pitch = 0.8-1.3 mm; slice thickness = 5-10 mm; matrix size 512 x 512; field of view 400 mm. The scans were obtained during the inspiration phase with patients in a supine position, approximately 2-3 weeks after PCR confirmation of COVID-19 positivity.

Pre-processing

In the pre-processing step, extraneous and irrelevant information was removed, resulting in more suitable images for the segmentation process. In this study, pre-processing steps were applied before deep neural network implementation to enhance the quality of chest CT images. The sequence of pre-processing steps included denoising, interpolation, and normalization to improve training data quality for deep learning algorithms. The denoising technique was utilized to minimize noise in images obtained from various scanners while preserving diagnostic image details and minimizing feature loss. Subsequently, all images were resampled to a $1 \times 1 \times 1$ size, followed by the application of Wavelet Decomposition (WAV) and Laplacian of Gaussian (LOG) filters. The LOG filter served to enhance image edges, with different sigma values being tested in three sizes, ranging from 0.5 to 5 pixels in increments of 0.5.

For noise removal, we employed the wavelet-based denoising technique. This method offers additional benefits, including ease of computation and full automation, as well as

applicability to various image processing tasks such as edge smoothing, detail enhancement, and compression.

In the normalization step, all pixel values were scaled to a range of 0 to 1. Subsequently, the dataset was divided into three groups: 60% for training, 20% for validation, and 20% for testing. To improve performance and minimize over fitting, data augmentation techniques were employed during training. Specifically, we applied random counter-clockwise rotations to lung images ranging from 10 to 359 degrees, and additional techniques such as zooming, and vertical and horizontal translocation. The augmented data were then used to train and validate the initial Mask R-CNN, 3D U-Net, and Caps Net architectures to learn lung and COVID-19 lesion volumes. The study was implemented on an NVIDIA GeForce RTX3080 GPU, running Python 3.8.10 and Torch 1.9.0+cu111.

Network architectures

Three frameworks; 3D-U-Net, Mask R-CNN, and Caps Net were used on international and Iranian cases for automated lung area segmentation. The goal of this segmentation was to identify COVID-19 lung lesions and segment them from the surrounding lung tissue. Caps Net is a technique inspired by the concept of 3D rendering in computer graphics and aims to encode image entities more intelligently. A published study experimentally showed the significance of using Caps Net on medical images compared to CNNs; Caps Net demonstrated its potential for improving performance in medical image analysis (30).

The Mask R-CNN architecture is composed of two primary components: Faster R-CNN and a parallel branch to predict per-pixel object class probabilities. We used the ResNet-101 backbone in the Faster R-CNN network to generate the feature maps passed to the region proposal network (RPN) and create a set of proposed regions that may contain lung lesions. Anchors corresponding to each area of interest are then passed through feature maps, generating masks that outline COVID-19 lung lesions on the input image. The task of COVID-19 lung lesion segmentation is formulated as a binary classification problem between the image background and lung lesions. The final output is a predicted mask corresponding to the input image, which can be overlaid on the input image for clinical use. To forecast the position (bounding box coordinates) of each item and localize each object separately from the others, Mask R-CNN employs the RPN block. As a result, for each designated item, the three attributes, i.e., bounding box, class, and mask are present (31).

Radiomics approach

During this phase, we extracted 867 radiomic features from the automatically segmented whole lung volume of the international and Iranian datasets using 3D Slicer software (www.slicer.org). To classify

COVID-19 patients using decision tree (DT), gradient-boosted decision tree (GBDT), and random forest (RF) machine learning classification algorithms, we applied three techniques, i.e., percentile selection, K-Best, and general univariate feature selection to select relevant features. This process helped reduce the number of optimal and efficient invisible features in developing models for diagnosing COVID-19 complications in the early stages of the disease which may be beyond human perception.

Evaluation metrics and equations

The evaluation metrics and quantitative analysis used in this study were as follows:

True positive (TP): The outcome where the model correctly predicts the positive class, meaning the sample is positive and the model predicted it as positive.

False negative (FN): The outcome where the model predicts the negative class, meaning the sample is positive but the model predicted it as negative.

False positive (FP): The outcome where the model predicts the positive class, meaning the sample is negative but the model predicted it as positive.

True negative (TN): The outcome where the model correctly predicts the negative class, meaning the sample is negative and the model predicted it as negative (Equations 1 to 6).

$$\text{specificity} = \frac{tn}{fp+tn} \quad (1)$$

$$\text{sensitivity} = \frac{tp}{tp+fn} \quad (2)$$

$$\text{precision} = \frac{tp}{tp+fp} \quad (3)$$

$$\text{accuracy} = \frac{tp+tn}{tp+tn+fp+fn} \quad (4)$$

$$\text{recall} = \frac{tp}{(tp+fn)} \quad (5)$$

$$F1 = \frac{2 \times (\text{precision} \times \text{recall})}{(\text{precision} + \text{recall})} \quad (6)$$

RESULTS

Tables 2 and 3 display the quantitative accuracy of automated segmentation of lungs and pneumonia lesions from chest CT images. It is evident that the 3D U-Net algorithm outperforms other methods in segmenting lungs and lesions. To determine the normality or abnormality of the images, three algorithms, i.e., Mask R-CNN, CNN, and Mask R-CNN+CNN were employed on DenseNet-161, ResNet-50, and ResNet-101 backbones. The ResNet-101 backbone yielded the most accurate results, achieving an accuracy of 82% for Mask R-CNN and

89% for Mask R-CNN+CNN (tables 4 and 5).

Table 6 presents the results of assessing the classification algorithms Mask R-CNN, CNN, and Mask R-CNN+CNN based on four metrics: accuracy, sensitivity, specificity, and area under the receiver operating characteristic (AUC) curve. The most effective algorithm in accurately classifying COVID-19 cases was Mask R-CNN+CNN, which achieved an accuracy of 96.39%.

Table 2. The result of lung segmentation with CapsNet, 3D U-Net and Mask-RCNN.

Lung Segmentation Methods	Dice Coefficient	Hausdorff distance
CapsNet	92.32 ± 0.93	0.96 ± 0.14
3D U-Net	93.66 ± 1.91	0.95 ± 0.74
Mask R-CNN	91.85 ± 2.34	0.87 ± 0.52

Table 3. The result of Covid-19 lung lesion segmentation with 3D U-Net and Mask R-CNN.

Lesion Segmentation Methods	Dice Coefficient	Hausdorff distance
3D U-Net	84.38 ± 3.89	0.90 ± 0.12
Mask R-CNN	81.03 ± 5.35	0.89 ± 0.24

Table 4. Comparison between the three backbones performance of Mask R-CNN.

Backbone	Accuracy (%)	Sensitivity (%)	Specificity (%)	AUC-ROC (%)
ResNet-50	81.90±5.83	77.67±11.66	96.24±7.43	88.90±8.99
ResNet-101	84.14±2.77	82.53±4.99	86.78±3.99	89.44±12.6
DenseNet-161	79.17±9.40	71.35±6.30	98.06±4.41	87.08±4.23

Table 5. Comparison between the different backbones performance of Mask R-CNN+CNN.

Backbone	Accuracy (%)	Sensitivity (%)	Specificity (%)	AUC-ROC (%)
ResNet-50	87.78±5.35	79.90±7.04	95.38±4.67	90.6±6.35
ResNet-101	89.15±3.11	85.94±6.75	89.30±2.90	92.5±7.48
DenseNet-161	87.9±2.81	76.60±5.43	97.85±4.75	88.44±3.92

Table 6. Quantitative evaluation of Covid-19 classification with Mask R-CNN, CNN and Mask R-CNN + CNN.

Method	Accuracy (%)	Sensitivity (%)	Specificity (%)	AUC-ROC (%)
Mask R-CNN	94.12±3.55	82.50±2.05	86.70±1.25	89.44±0.95
CNN	93.66±4.25	93.66±1.80	89.66±0.75	93.16±4.25
Mask R-CNN+CNN	96.39±2.94	85.90±2.25	89.31±3.15	92.24±0.10

The optimal subsets of radiomic features were ranked using three tree-based algorithms: DT, GBDT, and RF. The comparison results of ML models using four evaluation metrics (accuracy, sensitivity, specificity, and AUC) are presented in table 7. RF outperformed the other models in finding relevant features for COVID-19, achieving an accuracy of 91% for international and 92% for Iranian patients.

Table 8 illustrates the importance of relevant common features in both international and Iranian datasets for COVID-19 classification.

Table 7. The area under curve (AUC), accuracy, sensitivity, specificity for different classifiers used in two datasets.

Algorithms	AUC-ROC (%)		Accuracy (%)		Sensitivity (%)		Specificity (%)		Mean cross validation (%)	
	Nationality	International	Iranian	International	Iranian	International	Iranian	International	Iranian	International
RF	98.35±5.01	98.87±2.99	91.03±3.59	92.30±5.83	98.44±3.88	85.73±2/09	85.70±2.99	89.63±2.00	60.11±4.88	92.07±1.78
DT	94.06±4.80	84.09±1.96	83.7 5±5.11	84.53±3.21	97.58±1.98	80.20±4.92	60.17±5.33	85.16±1.68	62.55±4.31	92.09±2.99
GBDT	74.46±0.79	66.00±2.88	80.93±1.17	76.94±3.44	83.37±2.54	42.69±2.88	91.88±5.16	61.82±2.44	78.69±6.35	88.04±1.88

Table 8. The most common importance radiomic features that contributed to Covid-19 classifying in International and Iranian datasets.

Common radiomic features in both Iranian and International datasets			
Features	Feature Classes	Importance for Iranian dataset	Importance for International dataset
Difference Variance	Gray-Level Co-occurrence Matrix Features	0.474548	0.03125
Contrast	Gray-Level Co-occurrence Matrix	0.375885	0.02
Gray Level NonUniformity	Gray-Level Size-Zone Matrix Features	0.313935	0.02
Dependence NonUniformity Normalized	Gray-Level Dependence Matrix Features	0.279239	0.020833
Large Area LowGray Level Emphasis	Gray-Level Size-Zone Matrix Features	0.279239	0.01227
JointEntropy	Gray-Level Co-occurrence Matrix Features	0.02	0.01

DISCUSSION

The main focus of this paper was to showcase COVID-19 diagnosis systems that utilize CNN methods (figure 1). The results indicated the effectiveness of COVID-19 classification by deep learning algorithms such as Mask R-CNN, CNN, and Mask R-CNN+CNN with ResNeSt-50, ResNet-101, and DenseNet-161 as their backbones. Additionally, this study evaluated the efficacy of selecting relevant features for COVID-19 using three ML classifiers, namely DT, GBDT, and RF. Iranian and international datasets identified standard radiomic features of lungs which are associated with the classification of COVID-19 (table 2).

Predicting diseases such as COVID-19 can help control epidemic outbreaks and decrease economic costs. One of the most effective tools for discriminating between normal and abnormal cases and classifying the disease is the relevant features extracted from the region of interest. Previous studies have primarily utilized machine learning classification algorithms, data mining, and logistic regression methods to predict COVID-19. These studies often predicted the incidence of COVID-19 based on epidemiological data and related concepts (32-34). The current study focused on CT scan images and investigated radiomic features that may be associated with the COVID-19 pandemic in different nationalities.

Several literature reviews have compared different neural networks to determine the best one for COVID-19 classification based on accuracy and sensitivity. Based on the results, networks with ResNet, DenseNet, and ResNeXt as dense feature extractors have demonstrated the highest accuracy among several datasets (35-37).

In this study, similar to previous findings, a deeper ResNet-101 backbone outperformed competitors such as ResNet-50 as a backbone (36, 38). Furthermore, ResNet-101 demonstrated superior results compared to DenseNet-161, validating that it is more suitable as a backbone

network for COVID-19 detection (tables 5 and 6). The primary difference between DenseNet and ResNet lies in how they collect features. While ResNet collects features from shallower layers through summation, DenseNet achieves this through concatenation. ResNet introduces short connections to neural networks, which reduces the vanishing gradient problem and allows for much deeper network structures. Additionally, during feature extraction, short connections enable different combinations of convolution operators, creating many equivalent feature scales (39). Consequently, less critical marginal features are eliminated, and the network examines fewer features, resulting in more accurate classification.

This study demonstrates that the Mask R-CNN+CNN model can achieve a higher accuracy rate (96.4%) for COVID-19 classification. A reason why this framework performs better with deeper layers is that the classification model is established based on the bounding box determined from Mask R-CNN (table 6). Similarly, Podder *et al.* discovered that Mask R-CNN outperforms all other methods, delivering a specificity of 97.36% and an accuracy of 96.98%. Therefore, it can be considered an effective tool in healthcare (40). In addition, it has been noted that the Mask R-CNN technique shows promise in identifying diseases related to the chest. Ter-Sarkisov successfully trained a model that could quickly and easily adjust to new chest CT scan data, resulting in high sensitivity in diagnosing COVID-19 (41). Ramesh *et al.* (31) compared the performance of Mask R-CNN to Tang, Sun, and Li's U-Net segmentation architecture (42). The researchers discovered that Mask R-CNN outperformed U-Net, which was largely due to its distinctive structure. Unlike U-Net's contracting and expansive paths, Mask R-CNN employed recurring feature maps and included an RPN, which contributed to its superior performance. Additionally, the use of ResNet-101 as the backbone instead of ResNet-18 led to the deletion of less important features and examination of fewer features, resulting in improved accuracy of model

classification⁽³⁶⁾.

A study by Chen *et al.* describes the use of Mask R-CNN to extract lung outlines and lesion sites from CT images for COVID-19 detection⁽⁴³⁾. The model demonstrated high sensitivity and specificity for detecting COVID-19. In comparison, in the present study, the model of the Mask R-CNN+CNN was improved with a ResNet-101 backbone that achieved even higher accuracy than the original Mask R-CNN and CNN models. Note that deep learning models often require fine-tuning and optimization to achieve the best possible performance, and it seems that the authors of the present paper achieved better results by making improvements to their model architecture. Haque *et al.* created a CNN model that successfully detected COVID-19 from chest X-ray pictures with an accuracy of 97.56%⁽⁴⁴⁾. The proposed model with four convolutional layers performed better than models trained with three and five convolutional layers, achieving an accuracy of 99.1%, while keeping computational complexity to a minimum. Gunraj *et al.*⁽⁴⁵⁾ created COVID Net-CT, a deep convolutional neural network designed to identify COVID-19 from CT images. They employed an automated design exploration method to determine the optimal architecture for deep CNN. With an accuracy of 94.99%, this model was found to be superior to all others. However, SVM and naive Bayes models were discovered to be the most sensitive and specific models, with ratings of 93.34% and 94.30%, respectively, among all the other models. Furthermore, CovXNet, a deep learning model that employs depth-wise convolution to efficiently extract features from chest X-ray images, was developed by Mahmud *et al.* To recognize COVID-19 from a limited dataset, pre-trained convolutional layers were adjusted and directly implemented in the model. This method achieved an accuracy of 97.4% for binary classification and 90.02% for multi-class categories, which is the highest reported accuracy^(33, 46).

Wang⁽⁴⁷⁾ developed a deep learning model named COVID Net that correctly distinguished between conventional, non-COVID, and COVID-19 groups with an accuracy of 92.4%. Kundu *et al.*⁽⁴⁸⁾ presented their approach, COVID-SEGNET, which employs Mask R-CNN to detect ground glass opacities (GGOs) in chest CT scans of affected individuals. This technique is automated, does not need manual intervention, and achieves a high accuracy rate of 98.25% for classification and instance segmentation. In another investigation, Zheng *et al.*⁽⁴⁸⁾ proposed the use of a deep learning segmentation based on 3D U-Net to diagnose COVID-19 pulmonary infection. The use of this network presents great potential for diagnosing COVID-19, which is in line with our findings. Moreover, multi-class segmentation of lung and COVID-19 lung lesions has been found to be more effective using 3D U-Net, as indicated by other results^(49, 50). Nevertheless, identifying pneumonia lesions in

CT scans can be difficult as they significantly vary in appearance, size, shape, and location within the lung region, which is the primary challenge of 3D COVID-19 segmentation⁽⁵¹⁾.

The Convolutional Caps Net is an artificial neural network based on capsule networks, which was developed to identify COVID-19 from chest X-ray images using fewer layers. Similar to our experiment, this technique presents excellent performance for binary classification with a success rate of over 96% (97.24%); for multi-class categorization, it achieves a rate of 84.22%⁽⁵²⁾. These results confirm that capsule networks are effective in classification, even with limited data sets. Toraman *et al.* employed a different approach than CNN architectures by utilizing only four convolution layers, which is fewer in number, in addition to the primary capsule layer for detecting COVID-19 from CXR images⁽⁴⁹⁾. Capsule networks can also achieve favorable outcomes with several convolution layers, whereas CNN structures demand a higher number of layers.

Based on the aforementioned studies, extensive studies have created deep learning models that can effectively diagnose or classify the incidence of diseases, policies, and management of the spreading outbreak of coronavirus. However, due to the insignificance of the results obtained from these studies, pioneering research that requires less training time and higher computational power can be a viable strategy for developing future deep learning abnormality diagnosing methods, such as for COVID-19.

Although imaging has played an essential role in detecting and predicting diseases, medical images alone do not provide all the necessary information about patients with COVID-19. Therefore, intelligent imaging platforms that employ laboratory examination results, medical records, and clinical manifestations combined with imaging data can significantly improve detection and forecasting accuracy.

The performance evaluation of the three ML models conducted in this study revealed that the RF classifier had a greater ability to differentiate COVID-19 from normal cases compared to DT and GBDT, with an accuracy of $\geq 91\%$ and an AUC of ≥ 0.985 (table 7).

Random Forest (RF) builds multiple decision trees and merges their predictions to obtain a more accurate and stable forecast, rather than relying on individual trees⁽⁵⁰⁾.

Muhammad *et al.*⁽⁴⁷⁾ evaluated the efficacy of machine learning models in predicting COVID-19 infection using epidemiological data. Their results showed that the decision tree model had the highest accuracy rate of 94.99%, while the support vector machine model and Naïve Bayes model had the highest sensitivity (93.34%) and specificity (94.30%), respectively. In the present study, the RF

algorithm had a greater ability than DT to differentiate relevant COVID-19 radiomic features (table 6). In another study by Chen *et al.* (2020)⁽⁴³⁾, clinical and imaging features of COVID-19 were summarized as image changes, such as GGO, consolidation, air bronchi sign, paving stone sign, fibrous lesions, vascular thickening, and halo sign observed during CT scan examination. Furthermore, Shamout *et al.* have proposed a deep neural network for extracting features from informative areas of CXR images and a gradient-boosting model for learning from routine non-imaging clinical variables. These assist clinicians in predicting COVID-19 deterioration for patients in the emergency departments, with an AUC of 0.786. Their findings revealed that most CXRs do not exhibit airspace opacities. For these patients, non-respiratory complications, such as cardiovascular or neurological side effects may trigger further deterioration of COVID-19⁽⁵¹⁾. In Tang *et al.*'s study which employed quantitative features extracted from chest CT images, among the 30 quantitative traits examined, the volume of ground glass opacity regions (with a Hounsfield Unit range of -700 to -300) and their ratios with respect to the entire lung volume were found to be the most significant contributors to the severity of COVID-19⁽⁵²⁾. In the present study, three classifiers, namely decision tree (DT), gradient boosting decision trees (GBDT), and random forest (RF), were utilized to determine the importance of CT image features in COVID-19 classification.

To detect and forecast COVID-19 outcomes, several trials have employed radiomics. For example, Cai *et al.* (2020)⁽⁹⁾ demonstrated that CT radiomic characteristics were crucial to determining when RT-PCR would turn negative in COVID-19 patients. In their prediction model, there were 10 parameters, of which nine were CT radiomic characteristics. The five most critical radiomic features were original first-order minimum, original GLDM small dependence, original first-order maximum, original first-order 10 percentile, and low gray level emphasis. Large area high gray-level emphasis and original shape sphericity were also essential. Fu *et al.*⁽⁵³⁾ used radiomics and ML to predict the progression of initially stable COVID-19 infections. According to Wu *et al.* (2021)⁽⁵⁴⁾, CT texture characteristics could differentiate severe COVID-19 patients from those with other acute respiratory infections.

All CT images utilized in this study were obtained using different scanners and imaging protocols, and from patients at various stages of COVID-19 infection. Despite this variation, the results showed that six radiomic features (table 8), including difference variance, contrast, gray level non-uniformity, dependence non-uniformity normalized, large area, low gray level emphasis, and joint entropy were consistently identified as important discriminators of COVID-19 positive and negative patients in both

international and Iranian subjects. These six radiomic features, which are primarily gray texture features, were found to be closely associated with the pathological characteristics of COVID-19 infection and demonstrated strong diagnostic performance across different nationalities and imaging centers, despite variations in COVID-19 stages.

COVID-19 presents numerous challenges, including changes in lung lesions over time, volume involvement of the lung, and CT involvement severity score. Machine learning approaches can assist in determining the initial stages of lung involvement and the volume of lung affected. These tasks will be among our priorities going forward in medical diagnosis and decision-making. As demonstrated by similar studies, no computer-based detection system can claim 100% accuracy. To increase reliability, it is recommended that further laboratory examination results and clinical manifestations be combined with image data when developing clinical models.

CONCLUSION

The combination of Mask R-CNN and CNN with a ResNet-101 backbone achieved higher accuracy in classifying COVID-19 compared to CNN and Mask R-CNN alone. These results underscore the significance of common radiomic features in global databases, which provide excellent diagnostic value for COVID-19 classification. The study also suggests that a more extensive database is needed to enhance the robustness of the radiomic features and improve their influence on outputs.

ACKNOWLEDGEMENT

Thanks to Iran University of medical sciences and Qazvin University of medical sciences for their help and support.

Funding: This work was supported by the Research Chancellor of Iran University of Medical Sciences [Grant number 99-1-68-18262, Ethics Committee no: IR.IUMS.REC.1399.752,] in part by the Research Chancellor of Qazvin University of Medical Sciences [Grant number: 99-28-20-19413, Ethics Committee no: IR.QUMS.REC.1399.167].

Conflicts of interests: There is no conflict of interest.

Ethical consideration: Ethical approval was obtained for this study [Ethics Committee no: IR.QUMS.REC.1399.167, Approval date: 2020-08-15] and [IR.IUMS.REC.1399.752, Approval date: 2020-11-07].

Author contribution: S.C. and F.A.: conceived and designed. R.A., F.A., A.J.E. and E.R.N. collected the data. S.A. and A.A.T.Z. data processing and modeling. A.J.E. data analysis. Z.H-M. wrote the first draft of the manuscript. S.C., A.J.E. and Z.H-M. made the revision to the manuscript.

REFERENCES

1. Laino ME, Ammirabile A, Posa A, et al. (2021) The Applications of Artificial Intelligence in Chest Imaging of COVID-19 Patients: A Literature Review. *Diagnostics*, **11**(8): 1317.
2. Wang G, Zheng X, Zou Y, et al. (2023) CT imaging findings and clinical correlation analysis of different clinical types of novel coronavirus pneumonia %. *Int J Radiat Res*, **21**(1): 7-13.
3. Malguria N, Yen LH, Lin T, et al. (2020) Hussein A, Fishman EK. Role of Chest CT in COVID-19. *J Clin Imaging Sci*, **2021**(11): 30.
4. Li Y, Yao L, Li J, et al. (2020) Stability issues of RT-PCR testing of SARS-CoV-2 for hospitalized patients clinically diagnosed with COVID-19. *J Med Virol*, **92**(7): 903-8.
5. Santura I, Kawalec P, Furman M, Bochenek T (2021) Chest computed tomography versus RT-PCR in early diagnostics of COVID-19 - a systematic review with meta-analysis. *Pol J Radiol*, **86**: e518-e31.
6. Xie X, Zhong Z, Zhao W, et al. (2020) Chest CT for typical coronavirus disease 2019 (COVID-19) pneumonia: relationship to negative RT-PCR testing. *Radiology*, **296**(2): E41-E5.
7. Jain G, Mittal D, Thakur D, Mittal MK (2020) A deep learning approach to detect Covid-19 coronavirus with X-Ray images. *Biotechnology and Biomedical Engineering*, **40**(4):1391-405.
8. Zu ZY, Jiang MD, Xu PP, et al. (2020) Coronavirus disease 2019 (COVID-19): a perspective from China. *Radiology*, **296**(2): E15-E25.
9. Cai W, Liu T, Xue X, et al. (2020) CT quantification and machine-learning models for assessment of disease severity and prognosis of COVID-19 patients. *Academic radiology*, **27**(12):1665-78.
10. Sperrin M, Grant SW, Peek N (2020) Prediction models for diagnosis and prognosis in Covid-19. *British Medical Journal Publishing Group*; **2020**, 369.
11. Chung M, Bernheim A, Mei X, et al. (2020) CT imaging features of 2019 novel coronavirus (2019-nCoV). *Radiology*, **295**(1): 202-7.
12. Zhu Y, Gao Z-H, Liu Y-L, et al. (2020) Clinical and CT imaging features of 2019 novel coronavirus disease (COVID-19). *The Journal of Infection*, **81**(1): 147.
13. Shi H, Han X, Jiang N, et al. (2020) Radiological findings from 81 patients with COVID-19 pneumonia in Wuhan, China: a descriptive study. *The Lancet Infectious Diseases*, **20**(4): 425-34.
14. Ye Z, Zhang Y, Wang Y, et al. (2020) Chest CT manifestations of new coronavirus disease 2019 (COVID-19): a pictorial review. *European Radiology*, **30**(8): 4381-9.
15. Ling Z, Xu X, Gan Q, et al. (2020) Asymptomatic SARS-CoV-2 infected patients with persistent negative CT findings. *European Journal of Radiology*, **126**.
16. Liu R, Han H, Liu F, et al. (2020) Positive rate of RT-PCR detection of SARS-CoV-2 infection in 4880 cases from one hospital in Wuhan, China, from Jan to Feb 2020. *Clinica Chimica Acta*, **505**: 172-5.
17. Zhang H-t, Zhang J-s, Zhang H-h, et al. (2020) Automated detection and quantification of COVID-19 pneumonia: CT imaging analysis by a deep learning-based software. *European Journal of Nuclear Medicine and Molecular Imaging*, **47**(11): 2525-32.
18. Litjens G, Kooi T, Bejnordi BE, et al. (2017) A survey on deep learning in medical image analysis. *Medical Image Analysis*, **42**:60-88.
19. Panch T, Szolovits P, Atun R (2018) Artificial intelligence, machine learning and health systems. *Journal of global health*, **8**(2).
20. Amiri S, Akbarabadi M, Abdolali F, et al. (2021) Radiomics analysis on CT images for prediction of radiation-induced kidney damage by machine learning models. *Computers in Biology and Medicine*, **133**: 104409.
21. Lalmuanawma S, Hussain J, Chhakchhuak L (2020) Applications of machine learning and artificial intelligence for Covid-19 (SARS-CoV-2) pandemic: A review. *Chaos, Solitons & Fractals*, **139**: 110059.
22. Sear RF, Velásquez N, Leahy R, et al. (2020) Quantifying COVID-19 content in the online health opinion war using machine learning. *IEEE Access*, **8**: 91886-93.
23. Maghiddi HS, Asaad AT, Ghafoor KZ, et al. (2021) editors. Diagnosing COVID-19 pneumonia from X-ray and CT images using deep learning and transfer learning algorithms. *Multimodal Image Exploitation and Learning 2021*. International Society for Optics and Photonics.
24. Swapnarekha H, Behera HS, Nayak J, Naik B (2020) Role of intelligent computing in COVID-19 prognosis: A state-of-the-art review. *Chaos, Solitons & Fractals*, **138**: 109947.
25. Neri E, Miele V, Coppola F, Grassi R (2020) Use of CT and artificial intelligence in suspected or COVID-19 positive patients: statement of the Italian Society of Medical and Interventional Radiology. *La Radiologia Medica*, **125**(5): 505-8.
26. Grassi R, Belfiore MP, Montanelli A, et al. (2021) COVID-19 pneumonia: Computer-aided quantification of healthy lung parenchyma, emphysema, ground glass and consolidation on chest computed tomography (CT). *La Radiologia Medica*, **126**(4): 553-60.
27. Santos MK, Ferreira JR, Wada DT, et al. (2019) Artificial intelligence, machine learning, computer-aided diagnosis, and radiomics: advances in imaging towards to precision medicine. *Radiologia Brasileira*, **52**: 387-96.
28. Scapicchio C, Gabelloni M, Barucci A, et al. (2021) A deep look into radiomics. *La Radiologia Medica*, **126**(10):1296-311.
29. Lee Y, Hwang J-w, Lee S, Bae Y, Park J (2019) editors. An energy and GPU-computation efficient backbone network for real-time object detection. *Proceedings of the IEEE/CVF conference on computer vision and pattern recognition workshops*; 2019.
30. Jiménez-Sánchez A, Albarqouni S, Mateus D (2018) Capsule networks against medical imaging data challenges. *Intravascular imaging and computer assisted stenting and large-scale annotation of biomedical data and expert label synthesis*: Springer, **2018**: 150-60.
31. Ramesh V, Rister B, Rubin DL (2021) Covid-19 lung lesion segmentation using a sparsely supervised mask R-CNN on chest x-rays automatically computed from volumetric CTS. *ArXiv preprint arXiv*, **210508147**.
32. He X, Zhou C, Wang Y, Yuan X (2021) Risk assessment and prediction of COVID-19 based on epidemiological data from spatiotemporal geography. *Frontiers in Environmental Science*, **9**: 634156.
33. Muhammad L, Algehyne EA, Usman SS, et al. (2021) Supervised machine learning models for prediction of COVID-19 infection using epidemiology dataset. *SN Computer Science*, **2**: 1-13.
34. Tuli S, Tuli S, Tuli R, Gill SS (2020) Predicting the growth and trend of COVID-19 pandemic using machine learning and cloud computing. *Internet of Things*, **11**: 100222.
35. Song Y, Zheng S, Li L, et al. (2021) Deep learning enables accurate diagnosis of novel coronavirus (COVID-19) with CT images. *IEEE/ACM Transactions on Computational Biology and Bioinformatics*, **18**(6): 2775-80.
36. Ardakani AA, Kanafi AR, Acharya UR, et al. (2020) Application of deep learning technique to manage COVID-19 in routine clinical practice using CT images: Results of 10 convolutional neural networks. *Computers in Biology and Medicine*, **121**: 103795.
37. Liu B, Yan B, Zhou Y, et al. (2020) Experiments of federated learning for covid-19 chest X-ray images. *ArXiv Preprint arXiv: 200705592*.
38. Li Z, Peng C, Yu G, et al. (2018) Detnet: A backbone network for object detection. *arXiv preprint arXiv*, **180406215**.
39. He K, Zhang X, Ren S, Sun J (2016) editors. Deep residual learning for image recognition. *Proceedings of the IEEE conference on computer vision and pattern recognition*. Publisher: IEEE.
40. Podder S, Bhattacharjee S, Roy A (2021) An efficient method of detection of COVID-19 using Mask R-CNN on chest X-Ray images. *AIMS Biophys*, **8**: 281-90.
41. Ter-Sarkisov A (2022) Covid-ct-mask-net: Prediction of covid-19 from ct scans using regional features. *Applied Intelligence*. 2022:1-12.
42. Haiming T, Nanfei S, Yi L (2020) Segmentation model of the opacity regions in the chest X-rays of the Covid-19 patients in the us rural areas and the application to the disease severity. *medRxiv*, **10**(19): 20215483.
43. Chen H, Ai L, Lu H, Li H (2020) Clinical and imaging features of COVID-19. *Radiology of Infectious Diseases*, **7**(2): 43-50.
44. Haque KF, Haque FF, Gandy L, Abdalgawad A (2020) editors. Automatic detection of COVID-19 from chest X-ray images with convolutional neural networks. *2020 international conference on computing, electronics & communications engineering (ICCECE)*. IEEE.
45. Gunraj H, Sabri A, Koff D, Wong A (2022) COVID-Net CT-2: Enhanced deep neural networks for detection of covid-19 from chest ct images through bigger, more diverse learning. *Front Med*, **8**: 729287.
46. Mahmud T, Rahman MA, Fattah SA (2020) CovXNet: A multi-dilation convolutional neural network for automatic COVID-19 and other pneumonia detection from chest X-ray images with transferable multi-receptive feature optimization. *Computers in Biology and Medicine*, **122**: 103869.
47. Wang L, Lin ZQ, Wong A (2020) COVID-Net: a tailored deep convolutional neural network design for detection of COVID-19 cases from chest X-ray images. *Scientific Reports*, **10**(1): 19549.
48. Kundu A, Mishra C, Bilgaiyan S (2021) editors. Covid-segnet: Diagnosis of covid-19 cases on radiological images using mask r-cnn.

2021 Seventh International conference on Bio Signals, Images, and Instrumentation (ICBSII). IEEE.

49. Toraman S, Alakus TB, Turkoglu I (2020) Convolutional capsnet: A novel artificial neural network approach to detect COVID-19 disease from X-ray images using capsule networks. *Chaos, Solitons & Fractals*, **140**: 110122.

50. Ke G, Meng Q, Finley T, et al. (2017) editors. LightGBM: A highly efficient gradient boosting decision tree. NIPS; 2017.

51. Shamout FE, Shen Y, Wu N, et al. (2021) An artificial intelligence system for predicting the deterioration of COVID-19 patients in the emergency department. *npj Digital Medicine*, **4**(1): 80.

52. Tang Z, Zhao W, Xie X, et al. (2020) Severity Assessment of Coronavirus Disease 2019 (COVID-19) Using Quantitative Features from Chest CT Images. *Phys Med Biol*, **66**: 035015

53. Fu L, Li Y, Cheng A, et al. (2020) A novel machine learning-derived radiomic signature of the whole lung differentiates stable from progressive COVID-19 infection: A retrospective cohort study. *J Thorac Imaging*, **35**(6): 361-8.

54. Wu Z, Li L, Jin R, et al. (2021) Texture feature-based machine learning classifier could assist in the diagnosis of COVID-19. *Eur J Radiol*, **137**:109602.